Equation of state and pasta phases in neutron stars

Hong Shen *Nankai University, Tianjin, China*

申虹 南開大学 天津 中国

Collaborators:

Jinniu Hu *Nankai University, Tianjin, China*

Shishao Bao *Shanxi Normal University, China*

Xuhao Wu *Nankai University, Tianjin, China*

Fan Ji *Nankai University, Tianjin, China*

Contents

- Introduction
- EOS for neutron stars
- Nuclear pasta phases
- Hadron-quark pasta phases
- Summary

Introduction

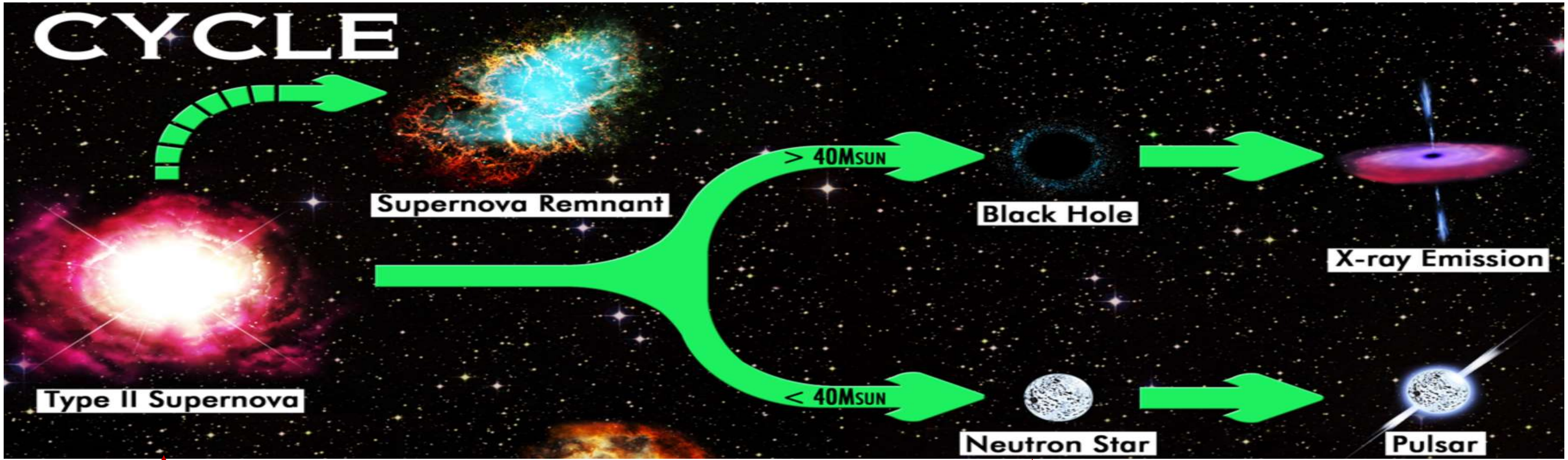

Equation of State (EOS)

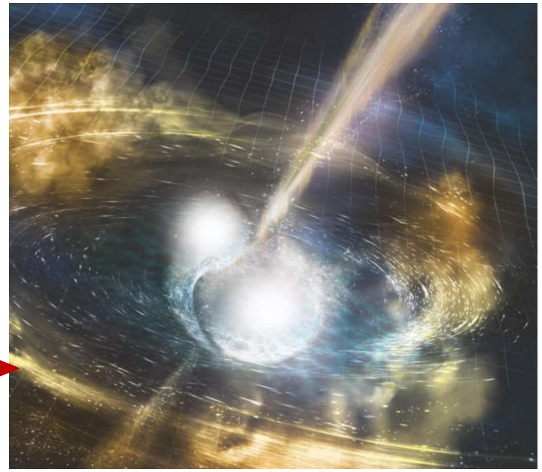

binary neutron stars merger

Classification of EOS

EOS for supernovae	EOS for neutron stars
temperature (T):	temperature (T):
0 ~ 100 MeV	**T = 0**
proton fraction (Yp):	proton fraction (Yp):
0 ~ 0.6	**β equilibrium**
construction:	construction:
nonuniform + uniform	**crusts + core**

EOS for supernovae

single nucleus approximation (SNA)

J. M. Lattimer and F. D. Swesty, Nucl. Phys. A 535, 331 (1991)

liquid-drop model with Skyrme force

H. Shen, H. Toki, K. Oyamatsu, K. Sumiyoshi, Prog. Theor. Phys. 100, 1013 (1998)

H. Shen, H. Toki, K. Oyamatsu, K. Sumiyoshi, Astrophys. J. Suppl. 197, 20 (2011)

Thomas-Fermi with RMF (TM1)

H. Togashi, K. Nakazato, Y. Takehara, S. Yamamuro, H. Suzuki, M. Takano, NPA 961 (2017) 78

Thomas-Fermi with realistic nuclear forces

nuclear statistical equilibrium (NSE)

M. Hempel and J. Schaffner-Bielich, Nucl. Phys. A 837, 210 (2010)

A.S. Botvina, I.N. Mishustin, Nucl. Phys. A 843, 98 (2010)

S. Furusawa, K. Sumiyoshi, S. Yamada, H. Suzuki, Astrophys. J. 772, 95 (2013)

S. Typel, G. Ropke, T. Klahn, D. Blaschke, H. Wolter, Phys. Rev. C 81, 015803 (2010)

G. Shen, C. J. Horowitz, E. O'Connor, Phys. Rev. C 83, 065808 (2011)

⋮

http://user.numazu-ct.ac.jp/~sumi/eos/index.html by K.Sumiyoshi

Home Page of Relativistic EOS table for supernovae

Table of Contents

- **Series of EOS tables based on the RMF framework**
  - Furusawa EOS (2016): Multi-composition of nuclei
    - Nuclear statistical equilibrium (NSE) treatment, extended from Shen EOS table
    - Smooth transition to uniform matter
    - Binding energy shifts for light nuclei
    - Improved shell corrections
  - Shen EOS (2011): Improved version of Shen EOS table:
    - With extended ranges & regular grid points
    - Sets without/with hyperons
  - Furusawa EOS (2011, 2013): Multi-composition of nuclei
    - Nuclear statistical equilibrium (NSE) treatment, extended from Shen EOS table
    - Smooth transition to uniform matter
  - Hyperon EOS (2008): Inclusion of strangeness
    - With hyperons and pions, extended from Shen EOS table
    - Sets with different hyperon-interactions
  - Shen EOS (1998)
    - Original version of Shen EOS table
- **Series of EOS tables based on microscopic approach**
  - Furusawa-Togashi EOS (2017): Multi-compotision of nuclei based on the variational many-body theory
    - Nuclear statistical equilibrium (NSE) treatment, extended from Togashi EOS table
    - Smooth transition to uniform matter
    - Binding energy shifts for light nuclei
    - Improved shell corrections
  - Togashi EOS (2017): Based on the variational many-body theory
    - Starting with realsitic nuclear forces
- **Series of EOS tables with quarks**

EOS for neutron stars

$T=0, \quad \rho \sim 10^{7} - 10^{15}\ \mathrm{g/cm^3}$

outer crust → inner crust → liquid core

$e+A \rightarrow e+n+A \longrightarrow (e,\mu)+(n,p) \rightarrow + \begin{cases} \text{hyperons} \\ \text{quarks} \\ \vdots \end{cases}$

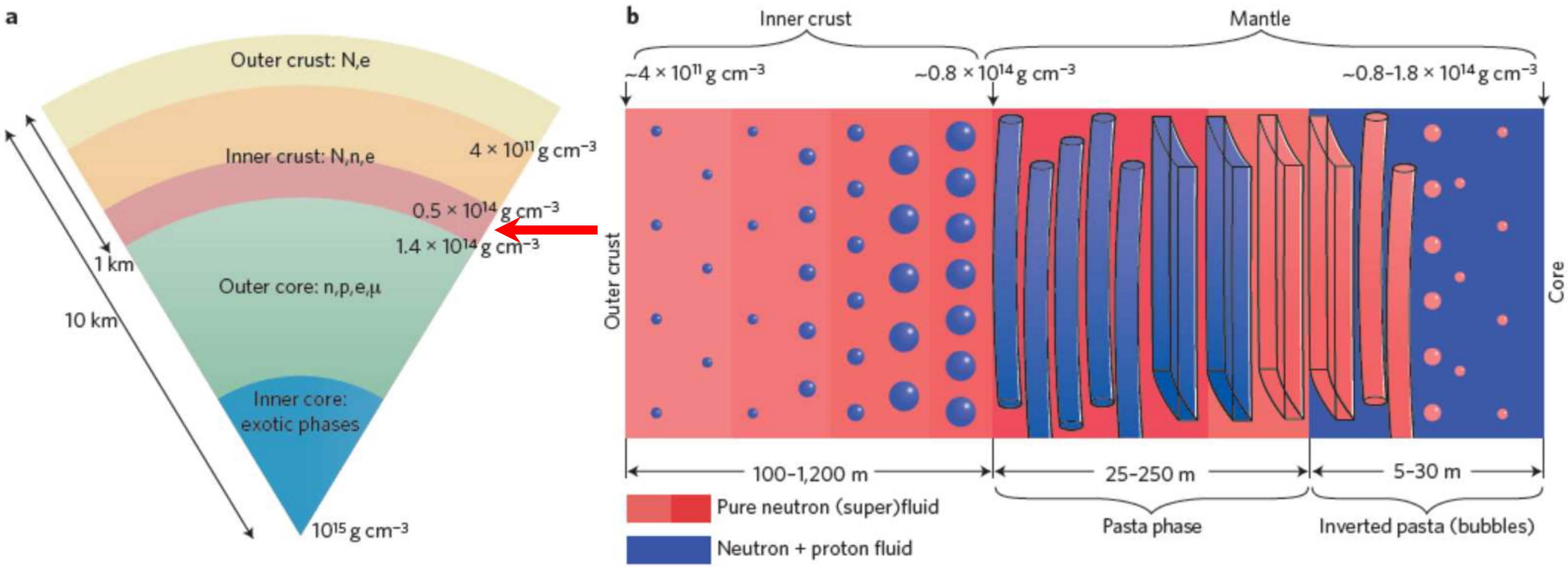

W. G. Newton, Nature Phys. 9 (2013) 396

EOS for neutron stars

unified EOS: crusts + core (consistent)

F. Douchin and P. Haensel, AA 380, 151 (2001)

liquid-drop model with Skyrme force

F. Fantina, N. Chamel, J. M. Pearson, and S. Goriely, AA 559, A128 (2013)

B. K. Sharma, M. Centelles, X. Vinas, M. Baldo, G. F. Burgio, AA 584, A103 (2015)

Thomas-Fermi with nonrelativistic nuclear models

H. Shen, PRC 65, 035802 (2002)

T. Miyatsu, S. Yamamuro, K. Nakazato, ApJ 777, 4 (2013)

M. Fortin, C. Providencia, Ad. R. Raduta et al., PRC 94, 035804 (2016)

Thomas-Fermi with realistic nuclear models

nonunified EOS: crusts + core (inconsistent)

M. Oertel, M. Hempel, T. Klahn, S. Typel, RMP 89, 015007 (2017)

Models used for EOS

- uniform matter
  at high density

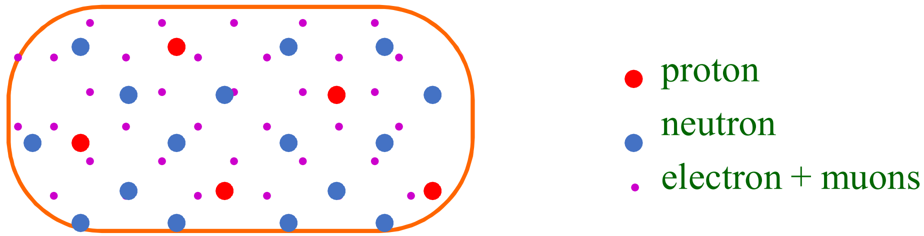

RMF (relativistic Mean Field)

- non-uniform matter
  at low density

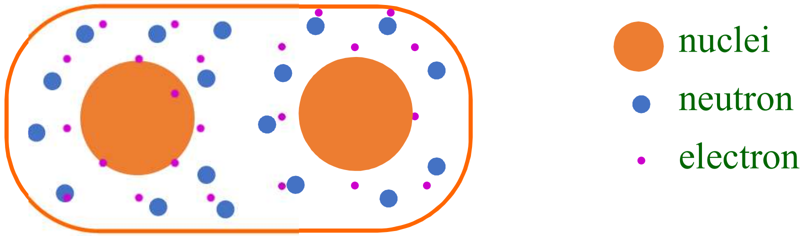

RMF + Thomas-Fermi approximation

Thomas-Fermi approximation

* body-centered cubic lattice
* parameterized nucleon distribution
* RMF input

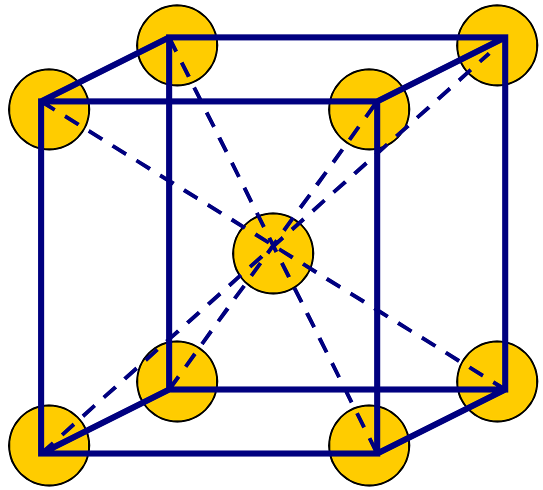

$$E = E_{bulk} + E_{surface} + E_{Coulomb} + E_{Lattice} + E_{electron}$$

assume states → *minimize free energy* → favorable state

RMF model

* generated RMF models with different L by turning g_ρ and Λ_v

$$
\begin{aligned}
\mathcal{L}_{\mathrm{RMF}} &= \bar{\psi}\left[i\gamma_\mu\partial^\mu - (M + g_\sigma\sigma) - \left(g_\omega\omega^\mu + \frac{g_\rho}{2}\tau_a\rho^{a\mu}\right)\gamma_\mu\right]\psi \\
&+\frac{1}{2}\partial_\mu\sigma\partial^\mu\sigma - \frac{1}{2}m_\sigma^2\sigma^2 - \frac{1}{3}g_2\sigma^3 - \frac{1}{4}g_3\sigma^4 \\
&-\frac{1}{4}W_{\mu\nu}W^{\mu\nu} + \frac{1}{2}m_\omega^2\omega_\mu\omega^\mu + \frac{1}{4}c_3\left(\omega_\mu\omega^\mu\right)^2 \\
&-\frac{1}{4}R_{\mu\nu}^a R^{a\mu\nu} + \frac{1}{2}m_\rho^2\rho_\mu^a\rho^{a\mu} + \Lambda_v\left(g_\omega^2\omega_\mu\omega^\mu\right)\left(g_\rho^2\rho_\mu^a\rho^{a\mu}\right)
\end{aligned}
$$

* all models have the same isoscalar saturation properties

TABLE II. Parameters g_ρ and Λ_v generated from the TM1 model for different slope L at saturation density n_0 with fixed symmetry energy $E_{\mathrm{sym}} = 28.05$ MeV at $n_{\mathrm{fix}} = 0.11\ \mathrm{fm}^{-3}$. The last two lines show the symmetry energy at saturation density, $E_{\mathrm{sym}}(n_0)$, and the neutron-skin thickness of ^{208}Pb, Δr_{np}. The original TM1 model has $L = 110.8$ MeV.

L (MeV)	40.0	50.0	60.0	70.0	80.0	90.0	100.0	110.8
g_ρ	13.9714	12.2413	11.2610	10.6142	10.1484	9.7933	9.5114	9.2644
Λ_v	0.0429	0.0327	0.0248	0.0182	0.0128	0.0080	0.0039	0.0000
$E_{\mathrm{sym}}(n_0)$ (MeV)	31.38	32.39	33.29	34.11	34.86	35.56	36.22	36.89
Δr_{np} (fm)	0.1574	0.1886	0.2103	0.2268	0.2402	0.2514	0.2609	0.2699

S. S. Bao, J. N. Hu, Z. W. Zhang, H. Shen, Phys. Rev. C 90 (2014) 045802

Symmetry energy effects

* energy per particle w as function of n and $\alpha = \frac{n_n - n_p}{n}$

$$w = w_0 + \frac{K_0}{18n_0^2}(n - n_0)^2 + \left[S_0 + \frac{L}{3n_0}(n - n_0)\right]\alpha^2$$

symmetry energy slope $L = \left[3n \frac{\partial E_{\rm sym}(n)}{\partial n}\right]_{n=n_0}$

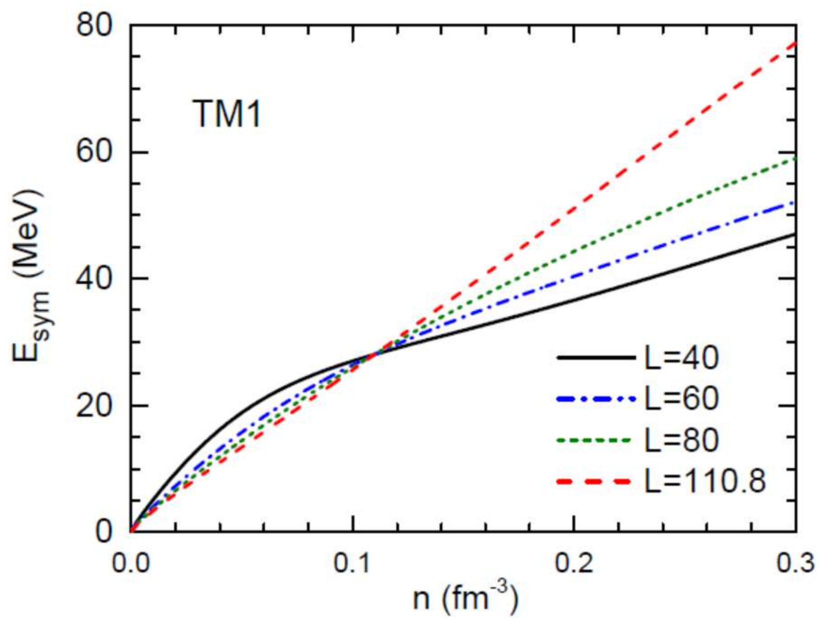

Nuclear pasta phases

crust-core transition

* **spinodal instability** (no surface and Coulomb)

  determined by the curvature of the free energy

* **bulk calculation** (no surface and Coulomb)

  phase equilibrium determined by the Gibbs conditions

* **coexisting phases (CP)** (surface and Coulomb perturbatively)

  phase equilibrium determined by the Gibbs conditions

* **compressible liquid-drop (CLD)** (minimization of free energy)

  phase equilibrium determined by minimization

* **Thomas-Fermi (TF)** (realistic description)

Methods for pasta phases

Coexisting phases (CP)

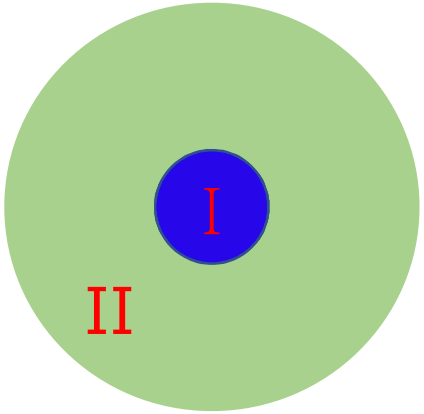

sharp
interface

Gibbs equilibrium

$$P^{\mathrm{I}} = P^{\mathrm{II}}$$
$$\mu_i^{\mathrm{I}} = \mu_i^{\mathrm{II}}$$

Thomas-Fermi (TF)

self-consistent
distribution

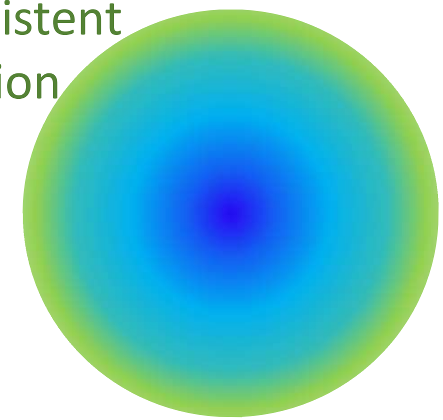

$$-\nabla^2\sigma + m_\sigma^2\sigma + g_2\sigma^2 + g_3\sigma^3 = -g_\sigma\left(n_p^s + n_n^s\right),$$
$$-\nabla^2\omega + m_\omega^2\omega + c_3\omega^3 + 2\Lambda_{\mathrm{v}} g_\omega^2 g_\rho^2 \rho^2\omega = g_\omega\left(n_p + n_n\right)$$
$$-\nabla^2\rho + m_\rho^2\rho + 2\Lambda_{\mathrm{v}} g_\omega^2 g_\rho^2 \omega^2\rho = \frac{g_\rho}{2}\left(n_p - n_n\right),$$
$$-\nabla^2 A = e\left(n_p - n_e\right),$$

perturbatively | Coulomb and surface energies | self-consistently

Symmetry energy ↔ pasta phases, crust-core

K. Oyamatsu, K. Iida, Phys. Rev. C 75, 015801 (2007)

B. A. Li, L. W. Chen, C. M. Ko, Phys. Rep. 464, 113 (2008)

F. Grill, C. Providência, S. S. Avancini, Phys. Rev. C 85, 055808 (2012)

Z. Zhang, L. W. Chen, Phys. Lett. B 726, 234 (2013)

S. S. Bao, H. Shen, Phys. Rev. C 89, 045807 (2014)

S. S. Bao, J. N. Hu, Z. W. Zhang, H. Shen, Phys. Rev. C 90, 045802 (2014)

S. S. Bao, H. Shen, Phys. Rev. C 91, 015807 (2015)

adjust g_ρ, Λ_V → fix symmetry energy at 0.11 fm^{-3}, different symmetry energy slope L →

- saturation property
- neutron star mass ~2 $M_\odot$
- finite nuclei

TM1 set →

L (MeV)	40.0	50.0	60.0	70.0	80.0	90.0	100.0	110.8
g_ρ	13.9714	12.2413	11.2610	10.6142	10.1484	9.7933	9.5114	9.2644
Λ_v	0.0429	0.0327	0.0248	0.0182	0.0128	0.0080	0.0039	0.0000

IUFSU set →

L (MeV)	47.2	50.0	60.0	70.0	80.0	90.0	100.0	110.0
g_ρ	13.5900	12.8202	11.1893	10.3150	9.7537	9.3559	9.0558	8.8192
Λ_v	0.0460	0.0420	0.0305	0.0220	0.0153	0.0098	0.0051	0.0011

Phase diagram of inner crust (TF)

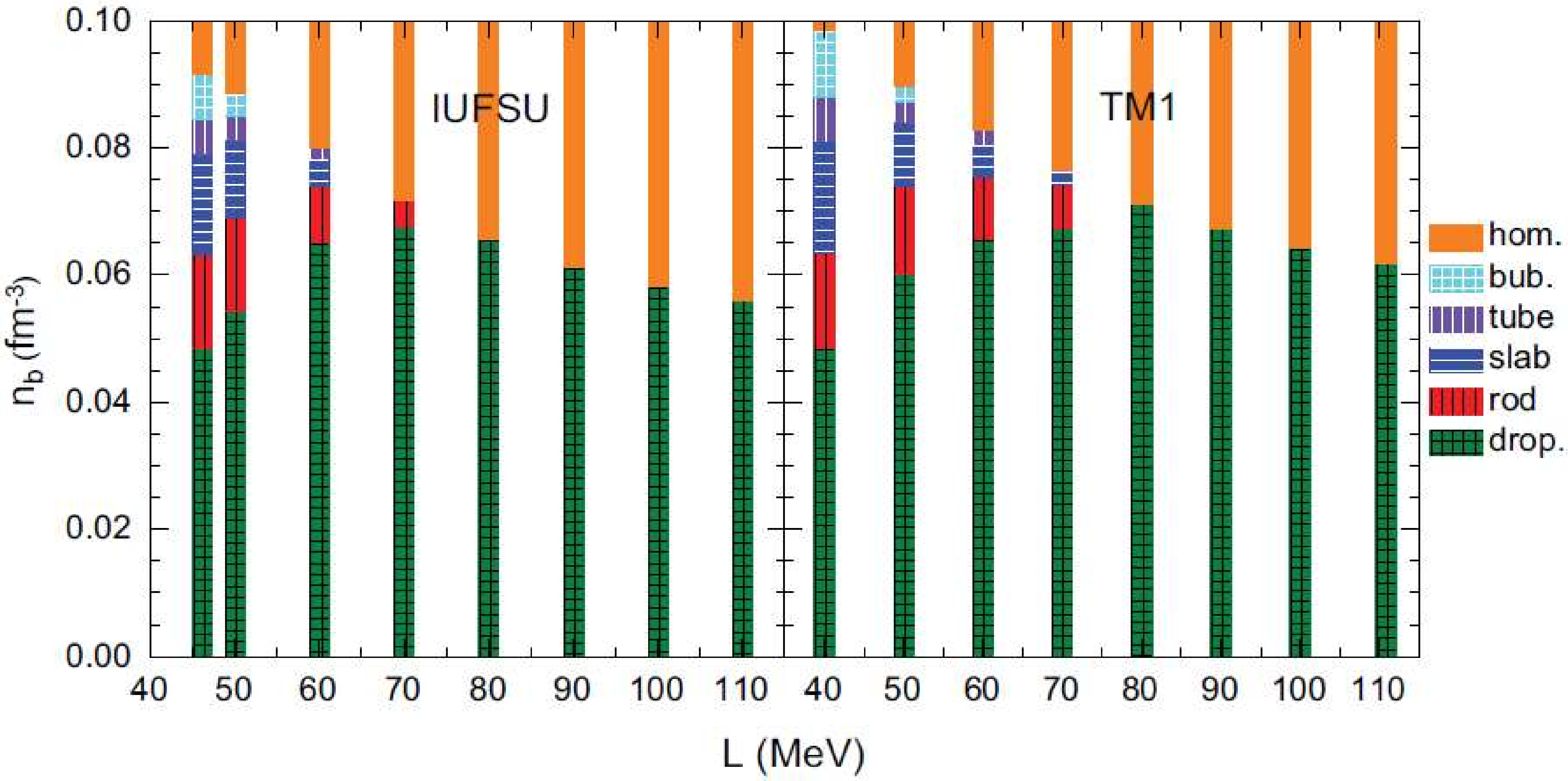

S. S. Bao, H. Shen, Phys. Rev. C 91, 015807 (2015)

smaller L corresponds to more pasta phases

smaller L corresponds to larger crust-core transition density

Pasta phase properties

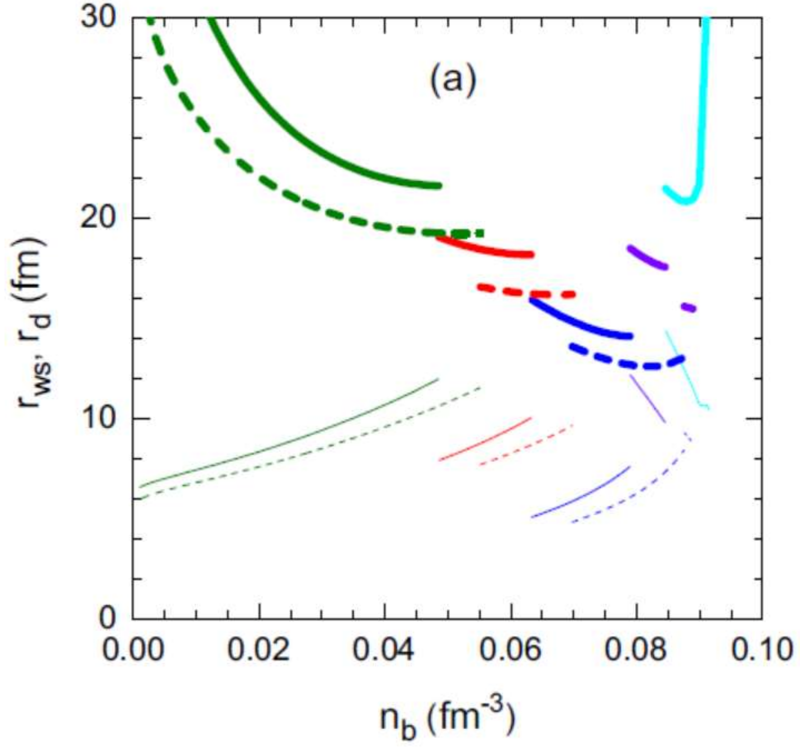

size of Wigner-Seitz cell
size of pasta structure

TF (solid lines) & CP (dashed lines)

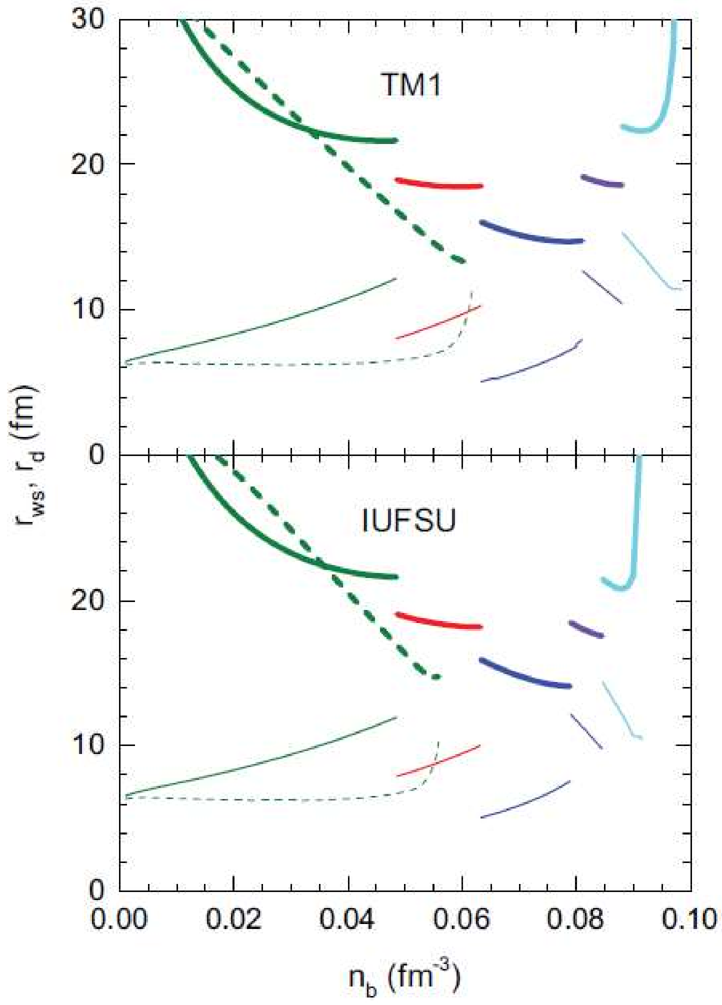

small L (solid lines)

large L (dashed lines)

Distributions of neutrons and protons

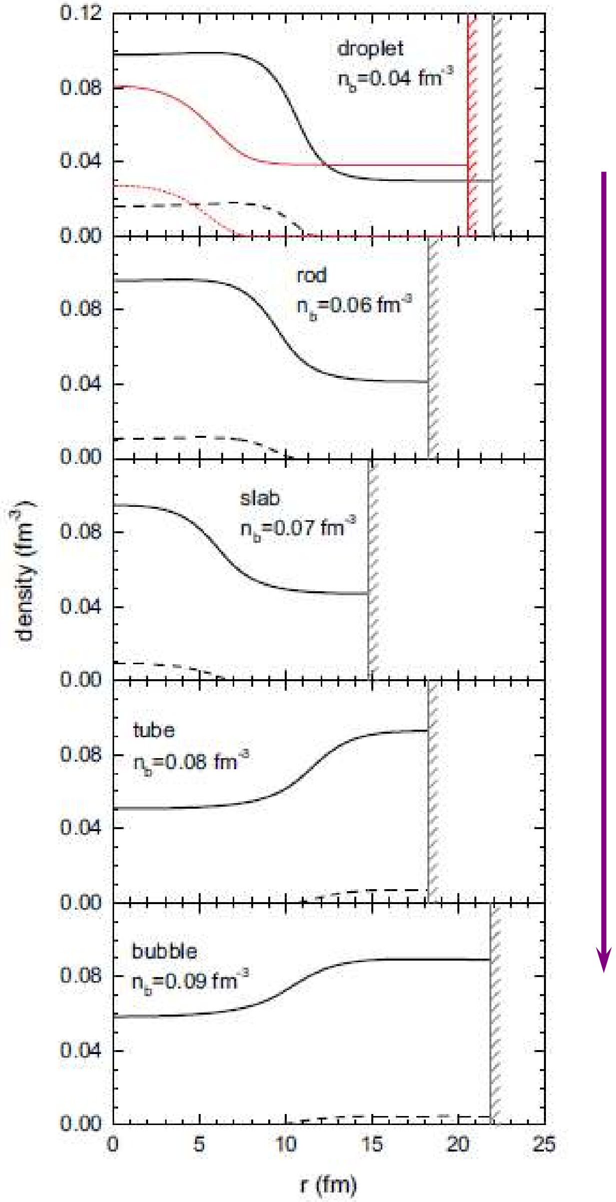

neutron
proton
L=110 MeV

neutron
proton
L=47.2 MeV

self-consistent Thomas-Fermi with the IUFSU model

S. S. Bao, H. Shen, Phys. Rev. C 91, 015807 (2015)

Crust-core transition

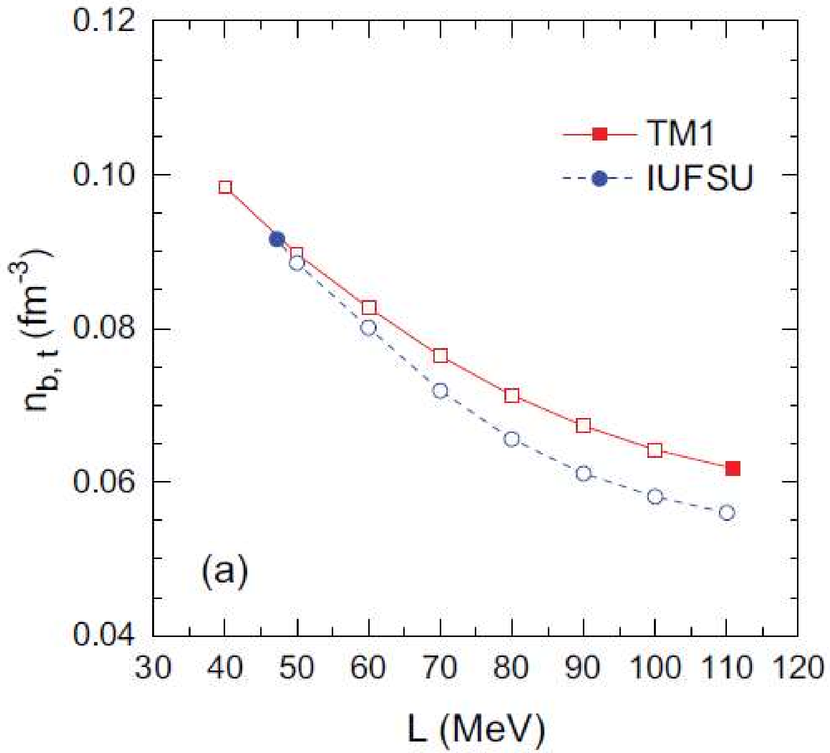

transition density

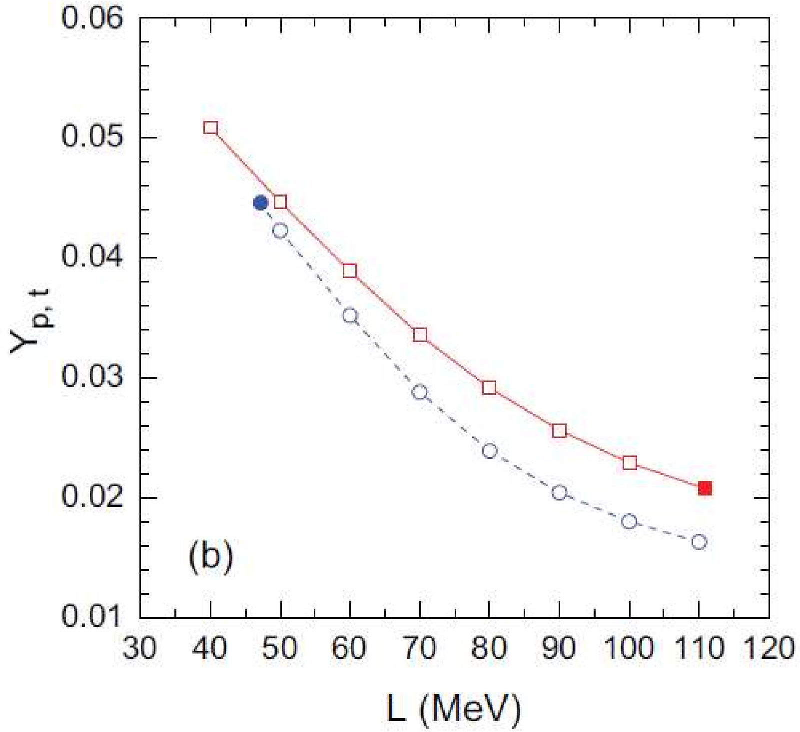

proton fraction

Neutron stars with unified EOS

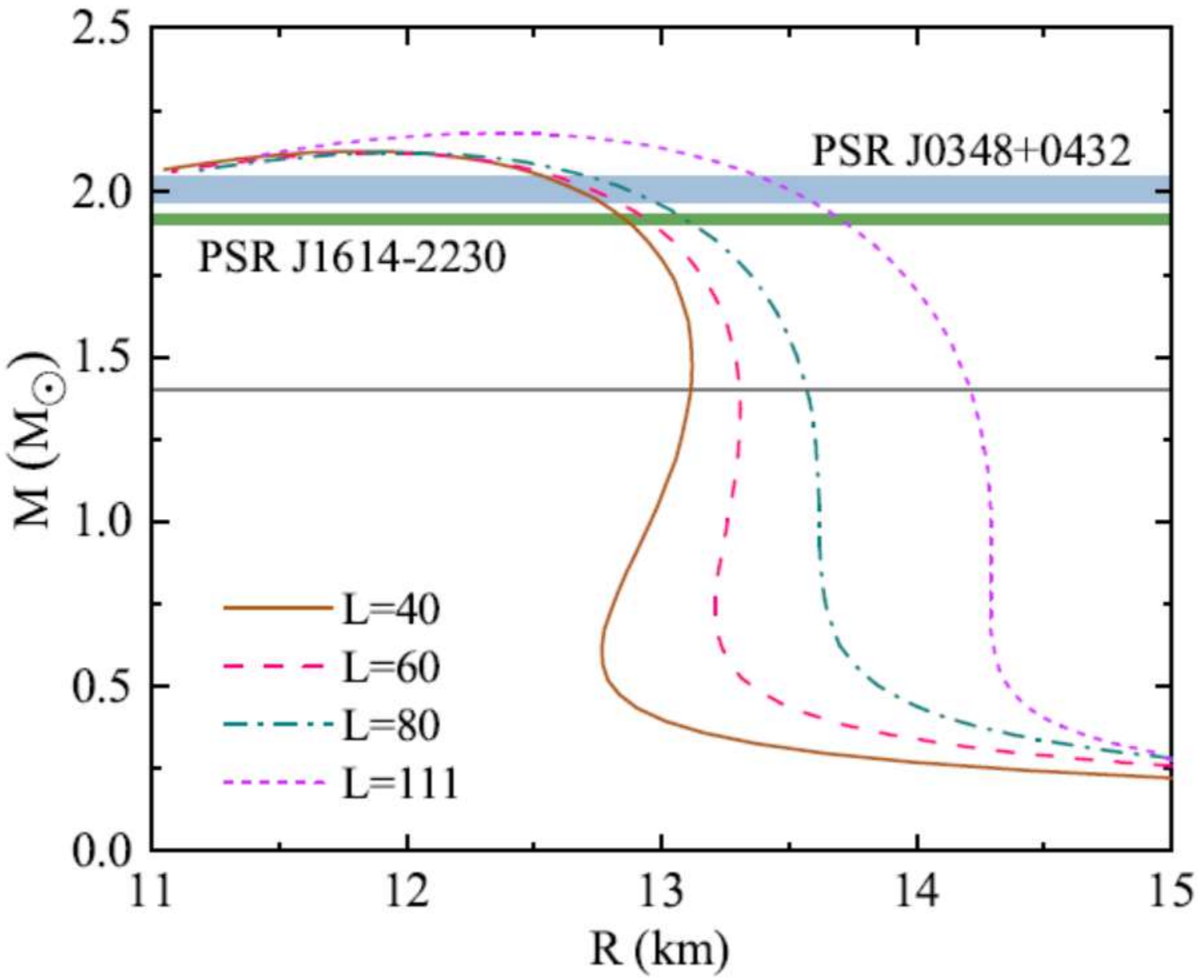

smaller L corresponds to smaller R

symmetry energy and neutron stars

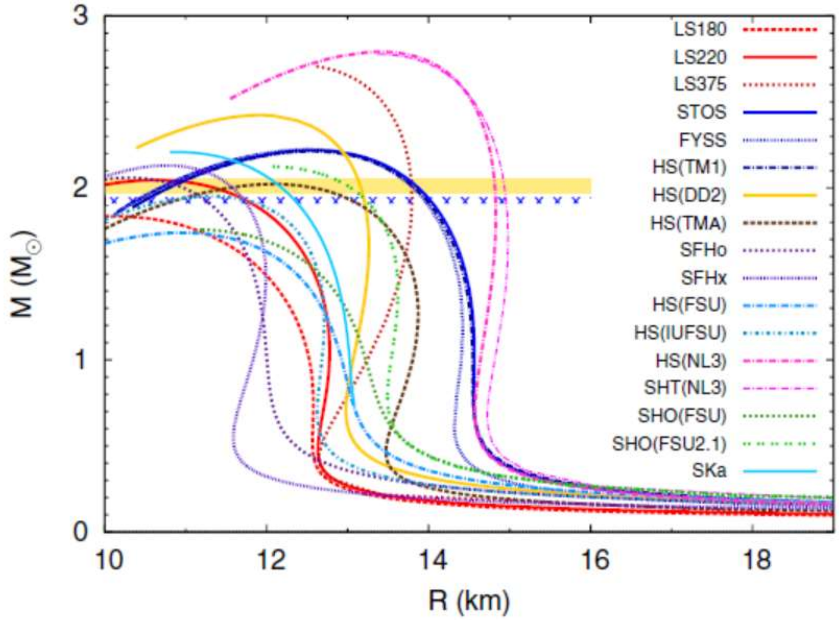

Nuclear interaction	n_{sat} (fm^{-3})	B_{sat} (MeV)	K (MeV)	Q (MeV)	J (MeV)	L (MeV)
SKa	0.155	16.0	263	−300	32.9	74.6
LS180	0.155	16.0	180	−451	28.6[a]	73.8
LS220	0.155	16.0	220	−411	28.6[a]	73.8
LS375	0.155	16.0	375	176	28.6[a]	73.8
TM1	0.145	16.3	281	−285	36.9	110.8
TMA	0.147	16.0	318	−572	30.7	90.1
NL3	0.148	16.2	272	203	37.3	118.2
FSUgold	0.148	16.3	230	−524	32.6	60.5
FSUgold2.1	0.148	16.3	230	−524	32.6	60.5
IUFSU	0.155	16.4	231	−290	31.3	47.2
DD2	0.149	16.0	243	169	31.7	55.0
SFHo	0.158	16.2	245	−468	31.6	47.1
SFHx	0.160	16.2	239	−457	28.7	23.2

M. Oertel, M. Hempel, T. Klähn, S. Typel, Rev. Mod. Phys. 89, 015007 (2017)

smaller L corresponds to smaller R

Hadron-quark psata phases

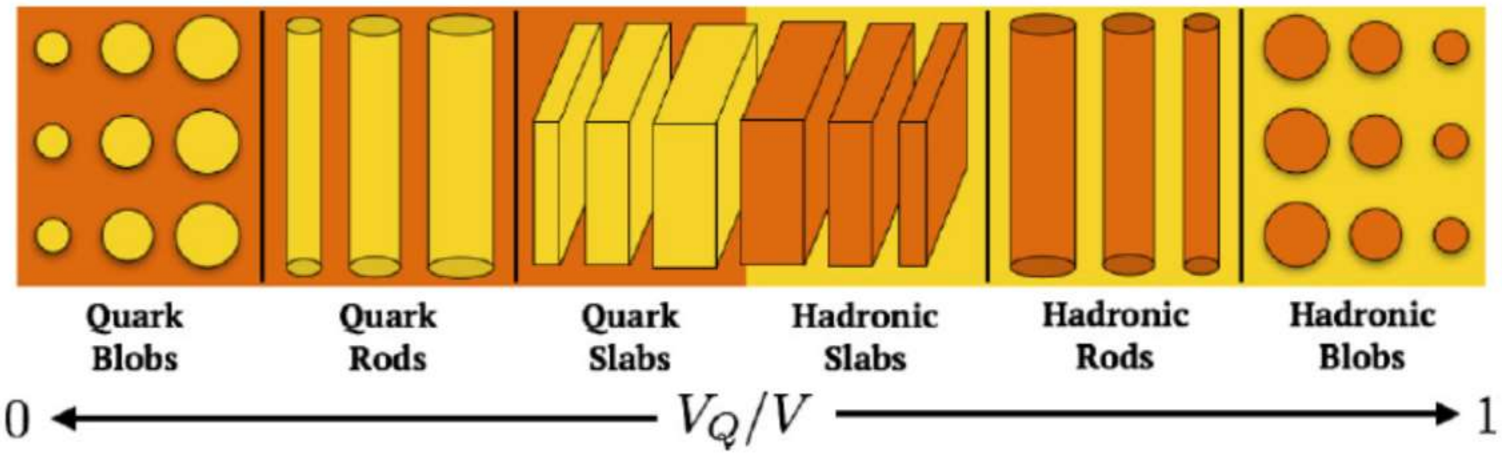

W. M. Spinella, F. Weber, G. A. Contrera, M. G. Orsaria, EPJA 52 (2016) 61

hadronic phase + quark phase

hadronic phase	quark phase
Brueckner-Hartree-Fock	MIT bag model
Relativistic mean-field	2-flavor NJL model
chiral effective field	3-flavor NJL model
:	:

Hadron-quark psata phases

NJL model

$$
\begin{aligned}
\mathcal{L}_{\rm NJL} &= \bar{q}\left(i\gamma_\mu\partial^\mu - m^0\right)q \\
&+G_S\sum_{a=0}^{8}\left[\left(\bar{q}\lambda_a q\right)^2 + \left(\bar{q}i\gamma_5\lambda_a q\right)^2\right] \\
&-K\left\{\det\left[\bar{q}\left(1+\gamma_5\right)q\right] + \det\left[\bar{q}\left(1-\gamma_5\right)q\right]\right\} \\
&-\underline{G_V}\sum_{a=0}^{8}\left[\left(\bar{q}\gamma^\mu\lambda_a q\right)^2 + \left(\bar{q}\gamma^\mu\gamma_5\lambda_a q\right)^2\right],
\end{aligned}
$$

Gap equation

$$
m_i^* = m_i^0 - 4G_S\langle\bar{q}_i q_i\rangle + 2K\langle\bar{q}_j q_j\rangle\langle\bar{q}_k q_k\rangle
$$

Hadron-quark pasta phases

hadron-quark mixed phase

$$\varepsilon_{\mathrm{MP}} = u\varepsilon_{\mathrm{QP}} + (1-u)\varepsilon_{\mathrm{HP}} + \varepsilon_{\mathrm{surf}} + \varepsilon_{\mathrm{Coul}}$$

$$\begin{aligned} \varepsilon_{\mathrm{surf}} &= \frac{D\sigma u_{\mathrm{in}}}{r_D}, \\ \varepsilon_{\mathrm{Coul}} &= \frac{e^2}{2}\left(\delta n_c\right)^2 r_D^2 u_{\mathrm{in}} \Phi\left(u_{\mathrm{in}}\right) \end{aligned}$$

$$\Phi\left(u_{\mathrm{in}}\right) = \begin{cases} \frac{1}{D+2}\left(\frac{2-D u_{\mathrm{in}}^{1-2/D}}{D-2} + u_{\mathrm{in}}\right), & D = 1, 3, \\ \frac{u_{\mathrm{in}}-1-\ln u_{\mathrm{in}}}{D+2}, & D = 2. \end{cases}$$

Hadron-quark pasta phases

* **Gibbs construction** (no surface and Coulomb)

  surface tension: $\sigma = 0 \quad \rightarrow \quad \varepsilon_{\rm surf} = 2\varepsilon_{\rm Coul} = 0$

  $$P_{\rm HP} = P_{\rm QP}, \quad \mu_n = \mu_u + 2\mu_d, \quad \mu_e^{\rm HP} = \mu_e^{\rm QP}$$

* **Maxwell construction** (no surface and Coulomb)

  surface tension: large σ $\rightarrow$ local charge neutrality $\rightarrow$ $\varepsilon_{\rm surf} = 2\varepsilon_{\rm Coul} = 0$

  $$P_{\rm HP} = P_{\rm QP}, \quad \mu_n = \mu_u + 2\mu_d, \quad \mu_e^{\rm HP} \neq \mu_e^{\rm QP}$$

* **coexisting phases (CP)** (surface and Coulomb perturbatively)

  phase equilibrium determined by the Gibbs conditions

* **energy minimization (EM)** (surface and Coulomb included in EM)

  phase equilibrium determined by energy minimization

Hadron-quark psata phases

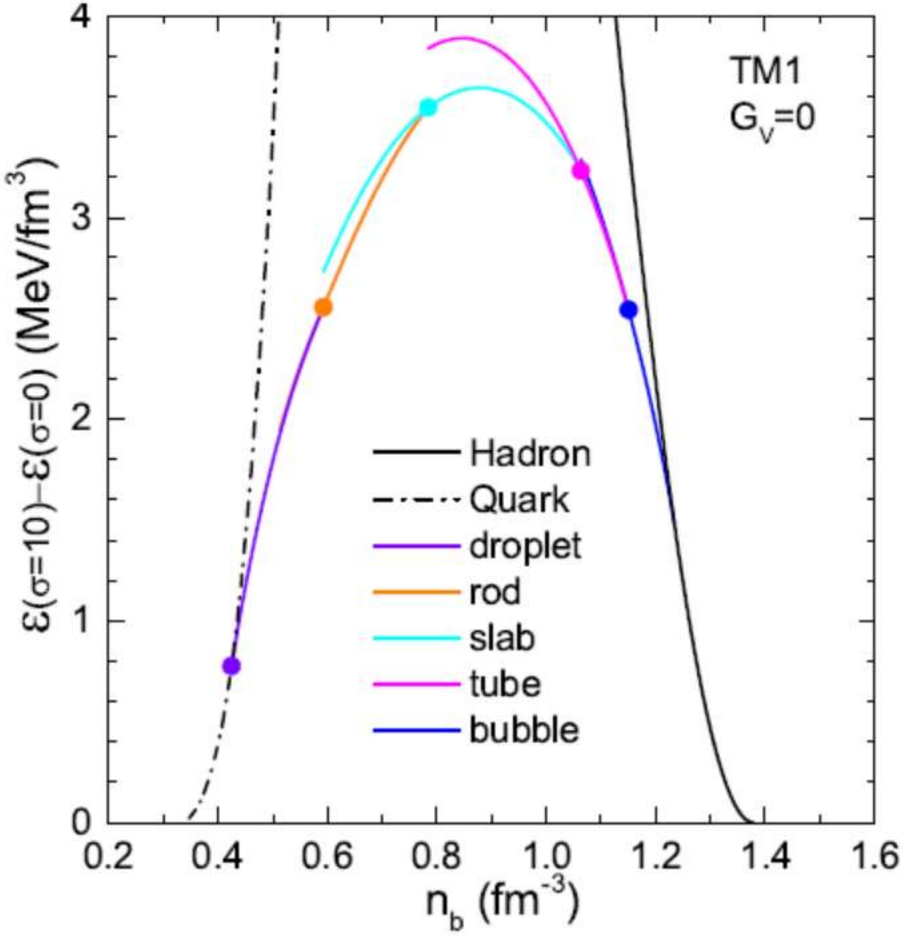

energy densities for pasta phases

X. H. Wu, H. Shen, arXiv:1811.06843

Hadron-quark psata phases

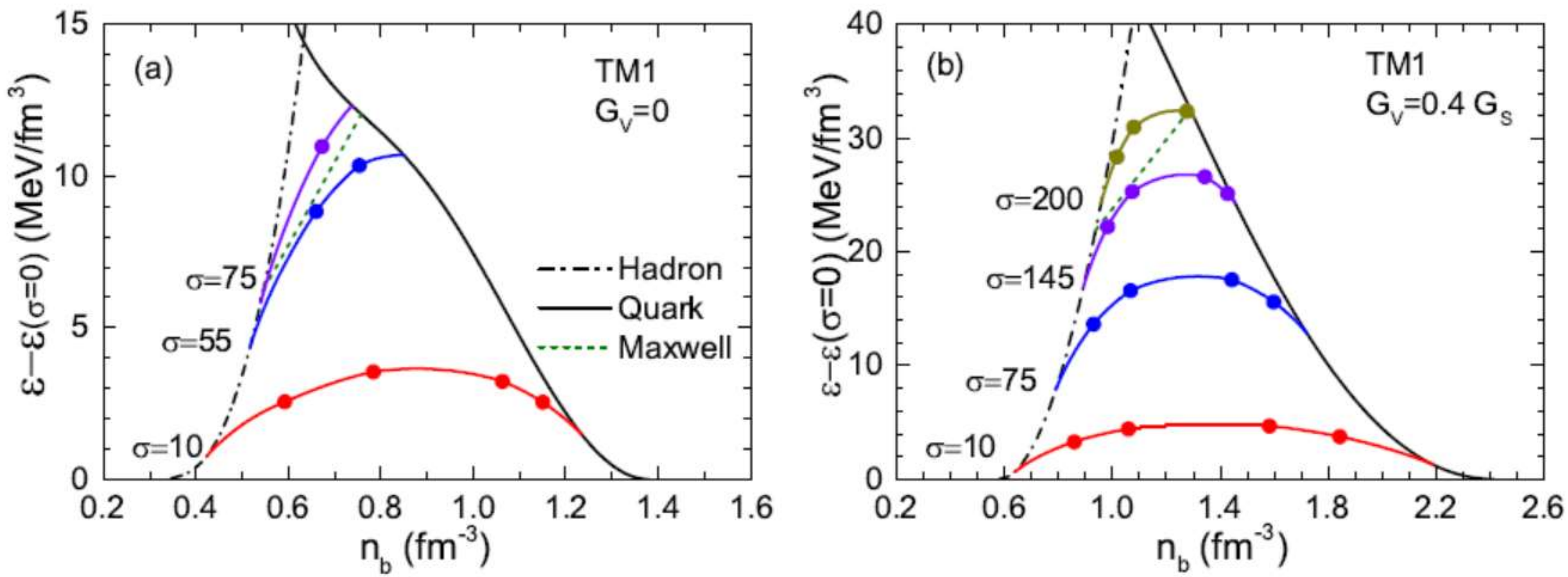

Gv=0 Maxwell construction is favored for $\sigma > 75$

Gv=0.4Gs Maxwell construction is favored for $\sigma > 200$

Hadron-quark psata phases

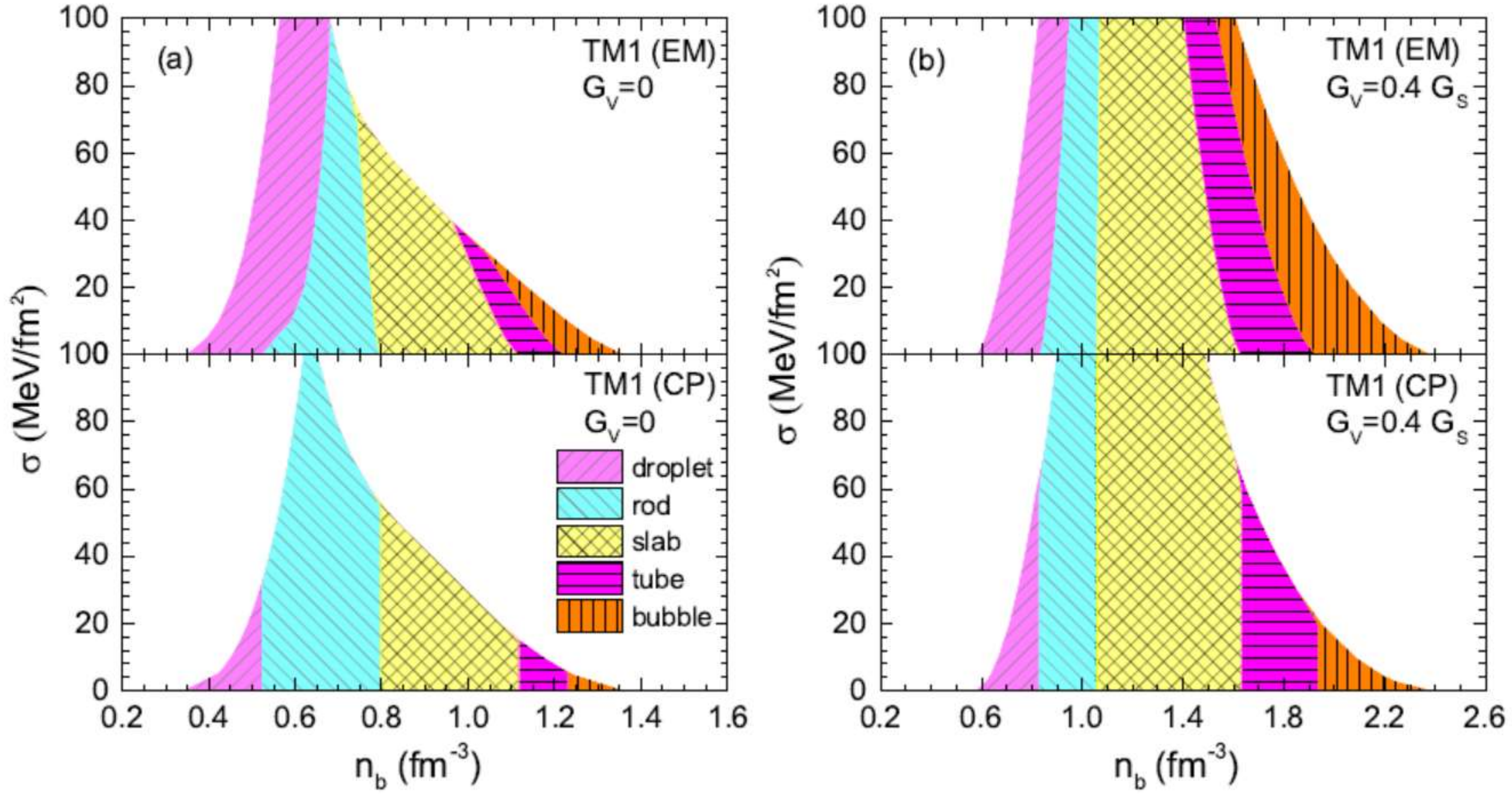

density ranges of pasta phases depend on σ

Hadron-quark psata phases

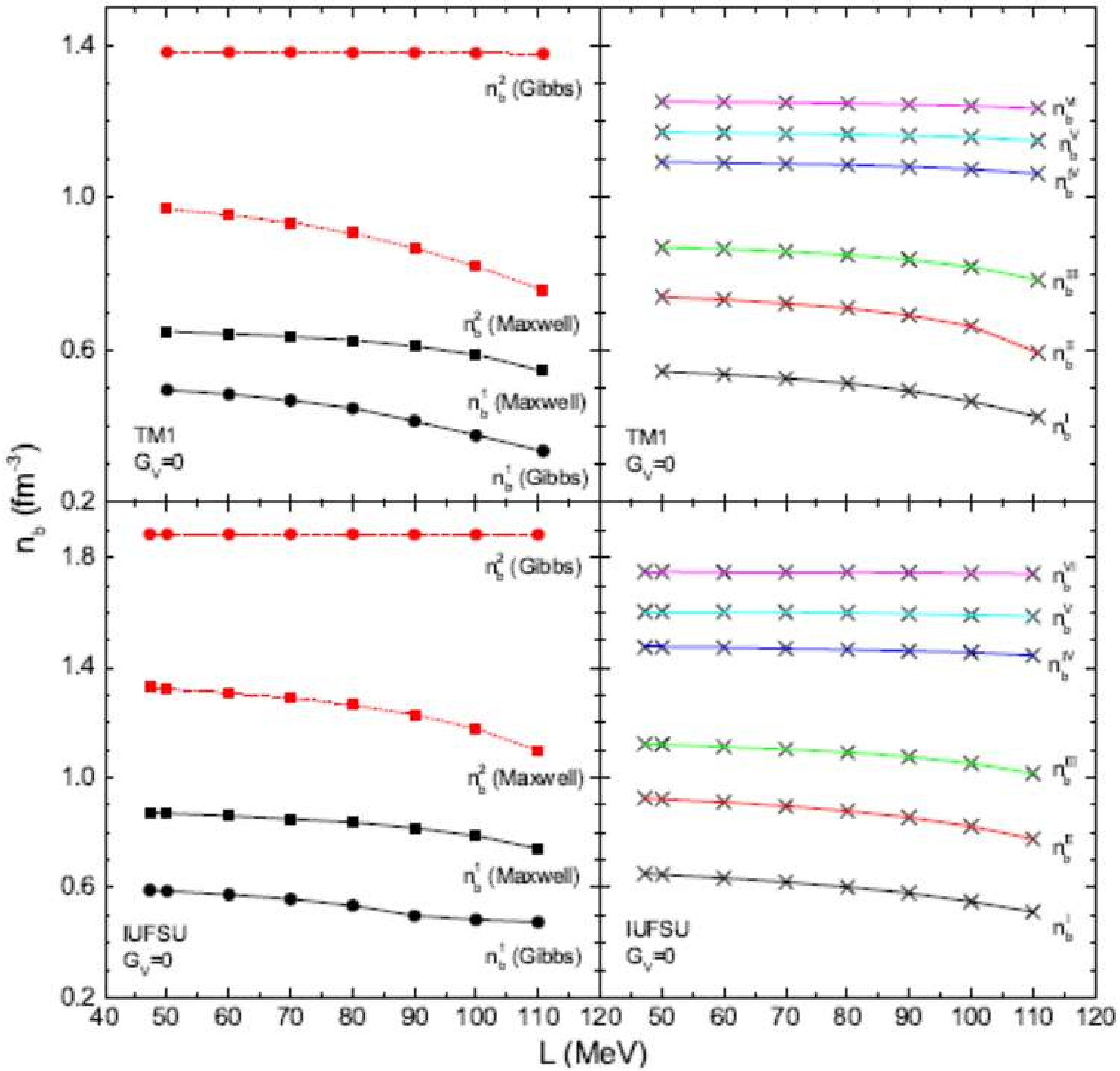

density ranges of pasta phases depend on L

EOS with quarks

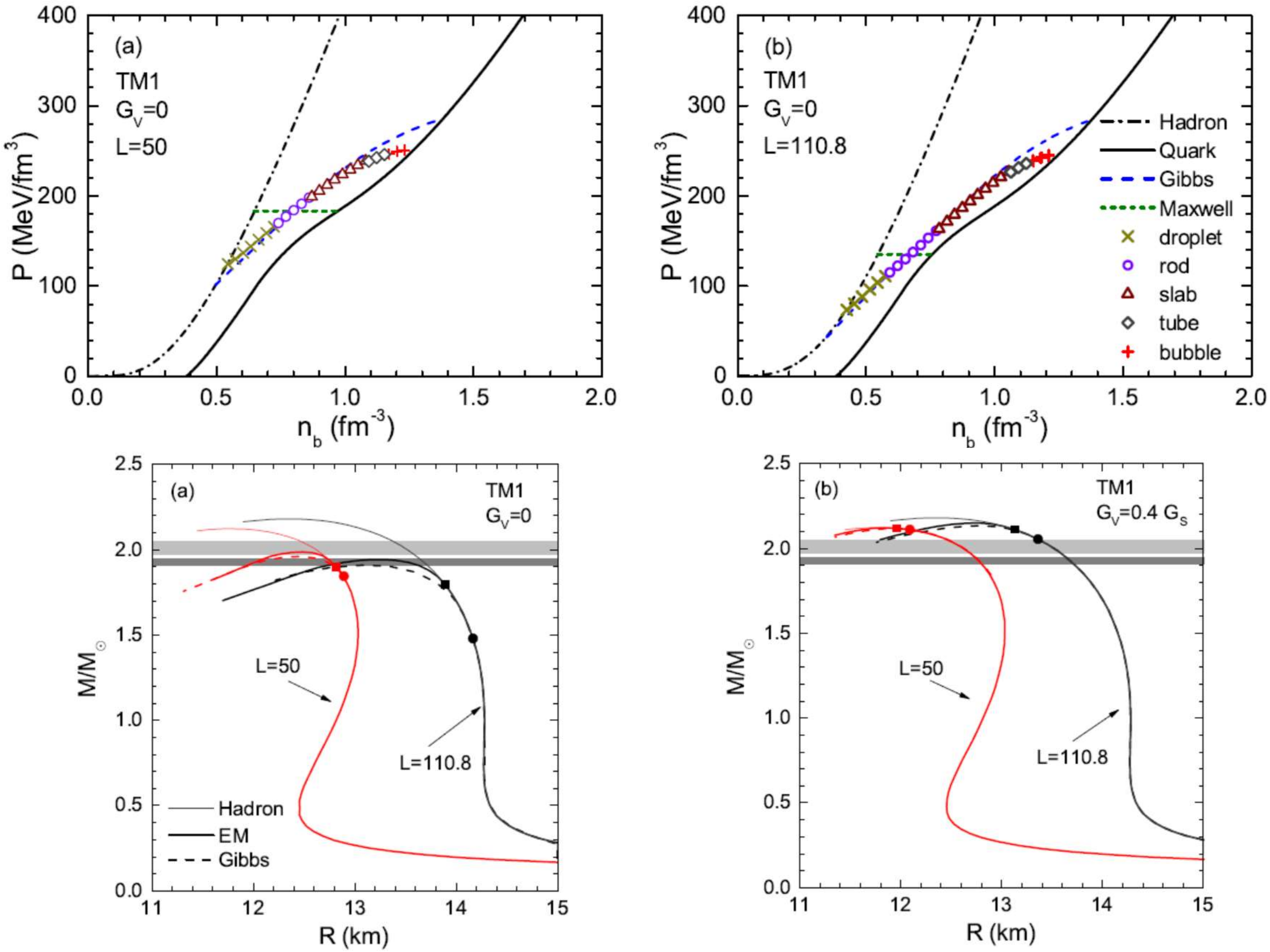

Summary

- Unified EOS is important for neutron stars
- Pasta phases in the inner crust depends on **L**
- Neutron-star radius is sensitive to **L**
- Hadron-quark pasta phases may exists
- Surface tension plays a key role